1   Title: Distinct neural mechanisms and temporal constraints govern a cascade of audiotactile

2   interactions

3   Abbreviated title: Audiotactile asynchronies elicit distinct effects

4

5   Johanna M. Zumer[1,2,3], Thomas P. White[1,2], Uta Noppeney[1,2,3]

6   [1]School of Psychology, University of Birmingham, Birmingham, B15 2TT, United Kingdom

7   [2]Centre for Computational Neuroscience and Cognitive Robotics, University of Birmingham,

8   Birmingham, B15 2TT, United Kingdom

9   [3]Centre for Human Brain Health, University of Birmingham, Birmingham, B15 2TT, United

10   Kingdom

11

12   Corresponding Author: Johanna Zumer, School of Psychology, University of Birmingham,

13   Birmingham, B15 2TT, United Kingdom; johanna.zumer@gmail.com

14   Number of pages: 36

15   Number of figures: 6

16   Number of words in Abstract: 250

17   Number of words in Introduction: 648

18   Number of words in Discussion: 1477

19   Conflict of Interest: The authors declare no competing financial interests.

24 **Abstract**

25 Synchrony is a crucial cue indicating whether sensory signals are caused by single or

26 independent sources. In order to be integrated and produce multisensory behavioural benefits,

27 signals must co-occur within a temporal integration window (TIW). Yet, the underlying neural

28 determinants and mechanisms of integration across asynchronies remain unclear. This

29 psychophysics and electroencephalography study investigated the temporal constraints of

30 behavioural response facilitation and neural interactions for evoked response potentials (ERP),

31 inter-trial coherence (ITC), and time-frequency (TF) power. Participants were presented with

32 noise bursts, 'taps to the face', and their audiotactile (AT) combinations at seven asynchronies:

33 0, ±20, ±70, and ±500 ms. Behaviourally we observed an inverted U-shape function for AT

34 response facilitation, which was maximal for synchronous AT stimulation and declined within a

35 ≤70 ms TIW. For ERPs, we observed AT interactions at 110 ms for near-synchronous stimuli

36 within a ≤20 ms TIW and at 400 ms within a ≤70 ms TIW consistent with behavioural response

37 facilitation. By contrast, AT interactions for theta ITC and ERPs at 200 ms post-stimulus were

38 selective for ±70 ms asynchrony, potentially mediated via phase resetting. Finally, interactions

39 for induced theta power and alpha/beta power rebound emerged at 800-1100 ms across several

40 asynchronies including even 500 ms auditory leading asynchrony. In sum, we observed neural

41 interactions that were confined to or extending beyond the behavioural TIW or specific for ±70

42 ms asynchrony. This diversity of temporal profiles and constraints demonstrates that

43 multisensory integration unfolds in a cascade of interactions that are governed by distinct neural

44 mechanisms.

45

46 **Significance Statement:**

47   Integrating information across audition and touch is critical for effective interactions with our

48   environment. We are faster to swat a mosquito when we perceive a prick on the skin together

49   with hearing the mosquito's buzzing. Importantly, we should integrate signals only when they

50   co-occur within a temporal integration window (TIW) and are hence likely to originate from a

51   common source. This psychophysics/electroencephalography study unravels a multitude of

52   neural interactions governed by different temporal constraints: interactions were confined to a

53   TIW for ERPs, specific for one particular asynchrony for inter-trial coherence, and extending

54   beyond the behavioural TIW for induced low frequency power. This diversity of temporal

55   profiles demonstrates that distinct neural mechanisms mediate a cascade of multisensory

56   integration processes.

57

Introduction

59   Imagine sitting outside on a summer evening. Suddenly you hear a buzz and then feel a prick to

60   your skin, as the mosquito lands. You are faster to swat it away because you first heard it

61   coming. This faster detection of a multisensory event is known as the redundant target effect

62   (RTE) (Miller, 1982, Diederich and Colonius, 2004, Sperdin et al., 2009) and illustrates the

63   enormous benefits of multisensory integration.

64   Importantly, we should integrate signals only if they arise from a common source but

65   segregate them otherwise. Synchrony is a critical cue for determining whether two signals come

66   from a common source. Multisensory need to co-occur within a certain tolerance of asynchrony,

67   termed a temporal integration window (TIW) (Diederich and Colonius, 2004). In particular, the

68   RTE typically follows an inverted U-shape function (Blurton et al., 2015) that is maximal for

69   (near)-synchronous signals and tapers off with increasing asynchrony thereby moulding the TIW.

70   Likewise, observers' perceived synchrony, the emergence of cross-modal biases, and perceptual

71   illusions follow a similar inverted U-shape function with its exact shape varying across different

72   behavioural measures and task-contexts (van Wassenhove et al., 2007, Megevand et al., 2013,

73   Berger and Ehrsson, 2014, Donohue et al., 2015).

74   At the neural level, multisensory influences have been identified in terms of response

75   enhancements and suppressions, super-additive and sub-additive interactions   (Meredith and

76   Stein, 1983, Stanford et al., 2005, Werner and Noppeney, 2010b), shortened neural response

77   latencies (Rowland and Stein, 2007) and altered neural representations (Fetsch et al., 2011, Rohe

78   and Noppeney, 2015, 2016). Evidence from neuroimaging, neurophysiology, and neuroanatomy

79   has shown that multisensory influences emerge at early and late stages of neural processing

80   (Foxe et al., 2000, Lutkenhoner et al., 2002, Murray et al., 2005, Senkowski et al., 2008, Sperdin

81   et al., 2009, Stekelenburg and Vroomen, 2009, Mercier et al., 2013, Mercier et al., 2015) nearly

82   ubiquitously in neocortex (Schroeder and Foxe, 2002, Ghazanfar and Schroeder, 2006, Lakatos

83   et al., 2007, Werner and Noppeney, 2010a, Ibrahim et al., 2016, Atilgan et al., 2018). They arise

84   already at the primary cortical level and increase progressively across the sensory processing

85   hierarchy (Foxe and Schroeder, 2005, Bizley et al., 2007, Kayser et al., 2007, Dahl et al., 2009).

86   This multi-stage and multi-site account of multisensory interplay raises the question of whether

87   the myriad of multisensory influences is governed by similar neural mechanisms and temporal

88   constraints. Further, how do those neural effects relate to the TIW defined by behavioural

89   indices? Given previous unisensory research showing an increase in the TIW along the sensory

90   processing hierarchy (Hasson et al., 2008, Kiebel et al., 2008), one may for instance hypothesise

91   that early multisensory interactions are confined to narrower temporal integration windows than

92   those occurring at later stages in higher order association cortices (Werner and Noppeney, 2011).

93   Moreover, recent neurophysiological studies suggest that multisensory interactions depend on

94   the phase of ongoing neural oscillations and/or rely on mechanisms of phase resetting. For

95   instance, Lakatos et al. (2007) showed that a tactile signal can reset the phase of ongoing

96   oscillations in auditory cortices, but only for specific asynchronies.

97   The current study aims to define the temporal constraints of multisensory interactions that can

98   be observed for evoked response potentials (ERP), inter-trial coherence (ITC), and induced

99   power responses and relate those to the TIW derived from behavioural response facilitation.

100   Participants were presented with brief airpuff noise bursts, 'taps to the face' and their

101   audiotactile (AT) combinations at seven levels of asynchrony: 0, ±20, ±70, and ±500 ms. In the

102   psychophysics study observers were instructed to respond to all A, T, and AT events in a

103   redundant target paradigm; in the EEG study a passive stimulation design was used to avoid

104   response confounds. We then identified multisensory influences in terms of multisensory

105   interactions (i.e. AT + No stimulation ≠ A + T) separately for each AT asynchrony level for

106   ERPs, ITC, and induced power responses and characterised their topography across post-

107   stimulus time.

108

Materials and Methods

109

110   *Participants.* Twenty-five healthy, adult participants with no neurological disorder were

111   recruited from the local university population (students as well as members of the general public)

112   (N=25, 12 female and 13 male; aged between 18-35 years old). One participant was excluded

113   due to an abnormal finding in the structural MRI. Two participants were excluded from the

114   behavioural analysis, because data were not collected for all conditions. Two different

115   participants were excluded from the EEG analysis, because insufficient EEG data were collected.

116   As a result we included 22 participants in both the behavioural and EEG analysis. They gave

117   written informed consent and were compensated either with cash or course credit.   Ethical

118   approval for the study was given by the University of Birmingham Science, Technology,

119   Engineering, and Mathematics Review Committee with approval number ERN_11-0429AP22B.

120   *Stimulation.* Tactile stimulation consisted of a touch to the left side of the face with 200 ms

121   duration. Tactile stimulation to the face was used as an ecologically valid stimulus that requires

122   a rapid response in everyday life. We also chose stimulation to the face (in contrast to hands), as

123   this body location does not require additional processing of being potentially crossed relative to

124   body position, thus potentially amenable to a quicker and more automatic route. The auditory

125   association areas that receive feed-forward (layer 4) input from somatosensory stimulation

126   appear to be optimally stimulated by cutaneous stimulation of the head and neck (Fu et al.,

127   2003). The left side was chosen based on previous findings that MSI is enhanced with left-side

128   stimulation and right hemisphere involvement (Giard and Peronnet, 1999, Downar et al., 2000,

129   Molholm et al., 2002, Hoefer et al., 2013). The part of the face touched was on/near the border

130   between the maxillary (V2) and mandibular (V3) divisions of the trigeminal cranial nerve. A

131   fibre optic cable (part of a fibre optic system: Keyence series FS-N, Neu-Isenburg, Germany)

132   was attached to a Lego pneumatic cylinder and driven to move by pressurised air. The tip of this

133   cable (3 mm diameter) was positioned near the face using a flexible plastic snap-together 'goose-

134   neck' pipe that was attached to an adjustable stand.   The air pressure changes were controlled by

135   a microcontroller connected via USB to the stimulus computer; communication to the

136   microcontroller was sent via serial port commands in MATLAB (Mathworks, Inc.).   The

137   duration of the open valve (i.e. when the diode was extended forward to touch the skin) was set

138   to 200 ms.   The fibre optic cable contained a dual fibre: one fibre projected light and the other

139   was a photodiode that detected the light reflectance; from this, the reflectance dynamics

140   confirmed the exact timing of the touch to the skin. This tactile apparatus was very similar to

141   that used by Leonardelli et al. (2015). After the experiment, subjects were queried as to whether

142   they could hear the tactile device moving prior to it touching them and none reported that they

143   could.

144   The auditory stimulus (target) was an airpuff noise of 200 ms duration. The volume of the

145   target was well above threshold for detection but not painfully loud; the volume was stronger on

146   the left channel than on the right (interaural intensity difference) to create the perception of

147   coming from the left. A constant background noise of a recording of a magnetic resonance

148   imaging   (MRI)   echo-planar   imaging   sequence   (obtained   from

149   http://cubricmri.blogspot.co.uk/2012/08/scanner-sounds.html) was played to help mask external

150   noises including those made by the tactile stimulator and for comparison with potential future

151   functional MRI studies. The volume of the background noise, equally loud in both ears, was

152   played at a level comfortable to participants and such that the tactile noises could not be heard.

153   All sounds were presented via E-A-RTone earphone (10 Ohm; E-A-R Auditory Systems) with

154   plastic tube connection (length = 75 cm) to foam ear insert (E-A-RLink size 3A), which also

155   acted as an earplug against external sounds.

156   *Experimental design.* Participants took part in one psychophysics and one EEG session on

157   separate days (typically 4-6 days gap). The experimental design and stimuli were identical across

158   the two sessions. In the psychophysics session participants responded to the first stimulus in a

159   trial irrespective of sensory modality, as fast as possible via a single key board button (i.e.

160   redundant target paradigm). In the EEG session, participants passively perceived the stimuli

161   without an explicit response in order to avoid motor confounds and allow for comparison with

162   sleep, non-responsive patients, etc.

163   In each session, participants were presented with the following trial types: no stimulus (or

164   null) condition (N), tactile alone (T), auditory alone (A), and seven audiotactile (AT) conditions

165   varying in asynchrony (-500 ms, -70 ms, -20 ms, 0 ms, 20 ms, 70 ms, 500 ms) where a 'negative'

166   asynchrony refers to A-leading-T (Fig. 1a). The audiotactile conditions are referred to by the

167   following abbreviations: AT500, AT70, AT20, AT0, TA20, TA70, TA500, respectively. These

168   asynchronies were chosen to fall either within the behaviourally-defined temporal integration

169   window (TIW) (≤70 ms) based on previous studies (e.g. (Navarra et al., 2007, Harrar and Harris,

170   2008, Nishi et al., 2014)) or outside the TIW (± 500 ms). Ten different trial types were

171   presented, interleaved randomly with an inter-trial interval uniformly distributed between 2.0 –

172   3.5 s, including both unisensory and audiotactile conditions with varying asynchronies between

173   the sensory stimuli. Each trial type was presented 100 times in each session. Trials were

174   presented in blocks of 250 trials (roughly 11.75 minutes) over four blocks separated by short

175   breaks. In the EEG session (performed about 1 hour before bedtime) we occasionally shortened

176   the blocks, but still presented 1000 trials in total. In the psychophysics session the AT500 and

177   TA500 conditions were not collected for two participants; thus for behavioural results, only the

178   data from the remaining twenty-two participants are included (after exclusion also of one

179   participant for the afore-mentioned structural MRI abnormality).

180   Participants kept their eyes closed to obliterate any visual input throughout the experiment.

181   They were seated comfortably with their head stabilised in an adjustable chin rest and were

182   requested to hold their head as still as possible (to promote spatial and temporal consistency of

183   the tactile stimulation over trials).

184   *EEG recording.* EEG data were recorded with a 64 channel BrainProducts MR-compatible

185   cap at 1000 Hz sampling rate, with 63 of the electrodes on the scalp. For all but the first three

186   participants, two additional bipolar electrodes were placed on the face to record horizontal EOG

187   and vertical EOG. For 17 participants, the 64th cap electrode was placed on the participants' back

188   for recording ECG. For the other 8 participants, the 64th electrode was instead placed on the

189   right (unstimulated) cheek for assistance as EOG/EMG. Signals were digitised at 5000 Hz with

190   an anti-aliasing filter of 1000 Hz, then down-sampled to 1000 Hz with a high-pass filter of 0.1

191   Hz and low-pass filter of 250 Hz. Electrode impedances were kept below 25 kOhm. Triggers

192   from the stimulus-control computer were sent via LabJack to the EEG acquisition computer.

193   *Tactile stimulation output*: The time course of light reflectance was assessed for each tactile

194   trial to ensure that i. the tactile device actually touched the skin and ii. to determine the touch

195   onset time (1000 Hz sampling rate). After computing the actual onset of the touch from the light

196   reflectance data, subsequently the exact multisensory onset asynchrony was computed for all

197   multisensory trials. Those that deviated by more than $\pm$ 5 ms from the desired asynchrony were

198   discarded. This resulted in 16.8% ($\pm$ 1.1%) and 16.4% ($\pm$ 1.2%) of trials rejected for the

199   behavioural and EEG data, respectively (N=24, after excluding the participant with structural

200   MRI abnormality).

201   *Behavioural analysis.* After exclusion of trials where touch was not applied or outside the

202   desired asynchrony, sensory trials were additionally discarded with no response or with response

203   times (RT) faster than 100 ms or slower than 1 s (occurring in total for an average of 2.7$\pm$1.1%

204   of trials across conditions). The median RT within a condition for each participant was

205   computed.

206   For each participant the *redundant target effect* (Hershenson, 1962) was computed for each

207   participant by subtracting the median RT of the AT condition at a particular level of asynchrony

208   from the fastest A or T condition with the onset of each unisensory condition adjusted for the

209   particular asynchrony (e.g. $RT_{AT20} - min(RT_T + 20$ ms $, RT_A)$. Using a one-sample two-sided t-

210   test we assessed whether the redundant target effect differed significantly from zero across

211   participants.

212   *EEG analysis: sleep staging.* To ensure that only EEG data was used in which participants

213   were awake, given the passive stimulation design with eyes closed and the evening acquisition,

214   standard sleep scoring was performed using American Academy of Sleep medicine (AASM)

215   2007   criteria   in   the   FASST   open-source   software

216   (http://www.montefiore.ulg.ac.be/~phillips/FASST.html) (Leclercq et al., 2011) and custom code

217   in MATLAB. Data were segmented into 30 s chunks and referenced to linked-mastoids. Sleep

218   stages were assessed by two of the authors (J.M.Z. and T.P.W.) independently with a

219   correspondence of 88%. Differences were discussed and a consensus reached (with

220   correspondence of the consensus to each assessor's scores at 93% and 94%). Any 30 s chunk

221   that was not scored as 'awake' was excluded from further analysis. If an individual participant

222   had fewer than 55 trials per condition remaining in the awake stage (prior to artefact rejection),

223   the participant was fully excluded. Two participants were excluded for this reason.

224   *EEG analysis: preprocessing:* All subsequent EEG data processing (after sleep staging) was

225   performed   using   the   open-source   toolbox   FieldTrip   (Oostenveld   et   al.,   2011)

226   (www.fieldtriptoolbox.org) and custom code in MATLAB. Eye movement artefacts were

227   automatically detected using three re-referenced bipolar pairs ('F7-F8', 'Fp2-FT9', and 'Fp1-

228   FT10') and the VEOG if available. These channels' data were band-pass filtered (1-16 Hz;

229   Butterworth, order 3) and transformed to z-values. The exclusion threshold was set at a z-value

230   of 6 and trials containing these artefacts were excluded. EEG data were re-referenced to the

231   average reference, high-pass filtered (0.2 Hz), band-stop filtered around the line noise and its

232   harmonics (49-51 Hz, 99-101 Hz, and 149-151 Hz), and epoched for each trial. Trials were

233   locked to the onset of the tactile stimulus for tactile and all multisensory conditions and to the

234   auditory or null trigger for A and N conditions, respectively. Initially, the epoch length was from

235   -1.5 s to 2.3 s. Then A trials were shifted ± 0.5, 0.07, 0.02, or 0 s before being added to a T trial,

236   to create the appropriate A+T combination to contrast with AT trials, hence resulting in variable

237   lengths of pre-stimulus and post-stimulus window lengths, depending on the AT asynchrony.

238   *EEG analysis: multisensory contrast.* Multisensory integration in the EEG data was identified

239   in terms of AT interaction, i.e. the sum of unisensory (A+T) contrasted to the audiotactile plus

240   null (AT+N). It is critical to add the null condition (to the multisensory) to account for non-

241   specific effects in a trial such as expectancy of stimulation as well as random noise. The sum of

242   unisensory (A+T) trials was computed for each AT asynchrony level such that the onsets of the

243   auditory and tactile stimuli were exactly aligned to the trials of the AT condition (i.e. we also

244   accounted for the jitter of tactile onsets, see above). Trials from each condition were randomly

245   sub-selected to ensure an equal number of trials per each of the four conditions in a given

246   contrast (A, T, AT, and N). To correct for multiple comparison (over channels, time, and, where

247   applicable, frequency) we performed cluster-based permutation tests for dependent (i.e. paired)

248   samples, with the sum of the t values (i.e. max sum) across a cluster as cluster-level statistic and

249   a cluster detected at an auxiliary uncorrected alpha threshold of 0.05.

250   *EEG analysis: multisensory effects on ERP, inter-trial coherence, and time-frequency power.*

251   For the evoked response potential (ERP) analysis, EEG data were low-pass filtered (40 Hz). The

252   average over trials within a participant was computed for the combination of conditions A+T and

253   AT+N separately. We assessed the AT interaction separately for each asynchrony level within a

254   500 ms time window, beginning at the onset of the second stimulus.

255   For time-frequency analysis, EEG data were Fourier transformed with separate parameters for

256   lower (4-30 Hz) and higher (30-80 Hz) frequencies. Sliding time windows of length equal to

257   four cycles (low frequencies) or 200 ms (high frequencies) at a given frequency in steps of 2 Hz

258   (low frequencies) or 5 Hz (high frequencies), after application of a Hanning taper (low

259   frequencies) or multitaper with +/- 7 Hz smoothing (high frequencies). The complex values

260   were kept for separate analysis of the inter-trial coherence (ITC) (also referred to as phase-

261   locking factor or phase-consistency index) and the time-frequency (TF) power magnitude. Note

262   that the sum of trials of different condition types (i.e. A+T and AT+N) was computed prior to

263   Fourier transformation so that any cancellation due to phase differences would occur prior to

264   obtaining the Fourier complex value (see Senkowski et al. (2007)). The ITC was computed for

265   each condition and subject as the absolute value of the sum of the complex values over trials. We

266   assessed the AT interactions for ITC and TF power separately for 'low frequency' and 'high

267   frequency' and for each asynchrony level, within a 1200 ms time window beginning at the onset

268   of the second stimulus and extending to include the low frequency (e.g. alpha and beta)

269   desynchronization / rebound effects.

270

271   **Results**

272   For the psychophysics study we report the redundant target effect as a behavioural index of

273   audiotactile integration for each asynchrony level. For the EEG data we report the multisensory

274   interactions (AT+N ≠ A+T) for ERPs, inter-trial coherence (ITC), and time-frequency (TF)

275   power. Both behavioural and neural indices of multisensory integration were identified

276   separately for each of the seven levels of AT asynchrony: 0, ±20, ±70, and ±500 ms (Figure 1a).

277   This allows us to investigate if the integration indices were i. limited to temporal integration

278   windows, ii. selective for specific asynchronies, or iii. symmetric for A-leading vs. lagging

279   asynchronies.

280

281   **Behavioural results: reaction time facilitation tapered by TIW**

282   As expected, we observed significantly faster (Figure 2 for p-values and t-values) response times

283   for the AT relative to the fastest unisensory condition (i.e. *redundant target effect*) for

284   asynchronies within a ≤ 70 ms window of integration (Figure 1b). Specifically, the RTEs (across

285   subjects mean ± SEM) for the different asynchrony levels were: AT70 = 35 ms ± 6 ms, AT20=

286   38ms ± 5 ms, AT0 = 35ms ± 4 ms, TA20 = 33ms ± 4 ms, and TA70 = 24ms ± 4 ms.

287   Surprisingly, we observed significantly slower response times for the AT500 relative to the

288   unisensory auditory condition, i.e. a negative redundant target effect (across subjects' mean ±

289   SEM) = -16ms ± 4 ms. In summary, our psychophysics study revealed that audiotactile

290   interactions within a 70 ms temporal integration window (TIW) facilitate stimulus processing

291   and response selection leading to faster response times.

292

293   **Audiotactile interactions for ERPs: limited to a TIW**

294   Figure 1C shows the ERPs for the A, T, AT and N conditions. Both tactile-alone (pink) and

295   auditory-alone (green) stimulation evoked a characteristic N100 followed by a P200, while the

296   null condition is a flat baseline. The tactile and auditory stimulation together generate the AT

297   evoked potentials across the different asynchrony levels (Figure 1C, black). While the influences

298   of both the tactile and auditory evoked responses are clearly visible in the AT responses, we can

299   also observe small deviations from the unisensory responses. In the following, we investigate

300   whether the AT+N responses deviate significantly from the sum of the A and T responses (i.e.

301   the AT interaction).

302   Figure 3 shows the ERPs for the sum over A+T (dark blue), sum over AT + N (light blue),

303   and the difference (A+T) – (AT + N), i.e. the audiotactile interaction effects across different

304   asynchrony levels. For ERPs we observed three AT interaction effects that differed in their

305   expression across levels of AT asynchrony (for significance of the test results, please see Figure

306   2).

307   The first AT interaction effect arose early, at about 100 ms post-stimulus, with a central

308   topography and was significant only for the synchronous condition (Figure 3, AT0 row).

309   Specifically, a modulation, during and after the N100 (70-170 ms), was found in both central and

310   posterior sensors, with the A+T greater than the AT+N during this time. We note that a trend for

311   this spatiotemporal effect was also observed for the AT20 condition.

312   The second AT interaction effect, where A+T was more negative than the AT+N, arose later

313   at about 370-400 ms mainly over posterior electrodes for AT asynchrony conditions within a ≤

314   20 ms temporal integration window (Figures 2, AT20, AT0, and TA20 rows). Even though this

315   AT interaction effect was significant only for AT20 and TA20, we observed a qualitatively

316   similar pattern for the synchronous AT0 condition.

317   The third AT interaction effect emerged at about 200 ms after the second stimulus (latency

318   range: 140-220 ms), was most pronounced over frontocentral electrodes, and was selective for

319   the asynchrony of ±70 ms (Figure 3, AT70 and TA70 rows). This AT interaction modulated the

320 shape and magnitude of the P200: the P200 occurred earlier and was reduced in amplitude for the

321 AT+N relative to A+T.

322 In summary, we observed three distinct AT interaction effects for ERPs that were expressed at

323 different AT asynchronies. Nevertheless, all AT interaction effects arose within the behavioural

324 ≤ 70 ms TIW, while no significant AT interactions were found for the AT500 or TA500

325 conditions.

326

327 **Audiotactile interactions for ITC: selective for ±70 ms asynchronies**

328 Figure 4 shows the ITC for the sum over A+T (light blue), sum over AT + N (dark blue), and the

329 difference (A+T) – (AT + N) (orange), i.e. the audiotactile interaction effects across different

330 asynchrony levels, as well as unisensory and null conditions separately. We observed significant

331 AT interactions for ITC in the theta band (4-8 Hz) specifically for ±70 ms asynchrony levels

332 (Figure 4, AT70 and TA70 rows; Figure 2 for significance test results). As shown in Figure 4,

333 the summed 'AT+N' ITC was greater than the summed 'A+T' for the auditory leading AT70,

334 but smaller for tactile leading TA70 condition. Thus, the direction of the audiotactile ITC

335 interaction depends on whether the auditory or the tactile sense is leading. The AT interaction

336 arose at about 200 ms post-stimulus and was most prominent over frontocentral electrodes,

337 mimicking the AT interactions we observed for the P200 in the ERP analysis (Figure 3B, AT70

338 and TA70 rows). In summary, the AT interactions for the theta-band ITC were selective for ±70

339 ms asynchronies and most likely associated with the ERP effects at the same post-stimulus

340 latency and asynchrony conditions.

341

342 **Audiotactile interactions for time-frequency power across AT asynchronies**

343   Figure 5 shows the TF power for the sum over A+T (light blue), sum over AT + N (dark blue),

344   and the difference (A+T) – (AT + N) (orange), i.e. the audiotactile interaction effects across

345   different asynchrony levels, as well as unisensory and null conditions separately. For

346   significance test results, see Figure 2.

347   *Theta power*: Both auditory and tactile stimuli induced theta power peaking at about 200 ms

348   post-stimulus primarily over fronto-central electrodes (Figure 5; Unisensory row). This peak in

349   theta power corresponds to the P200 (Figure 3) in the ERP analysis and an increase in ITC

350   (Figure 4). Note that our data illustrate the point that the 'A+T' sum (Figure 5: AT0 light blue),

351   which was computed by first summing trials before frequency transformation according to

352   Senkowski et al. (2007), is indeed different than if the power of the tactile (Figure 5: Unisensory

353   pink) and auditory (Figure 5: Unisensory green) had first been computed and then summed.

354   We observed significant AT interactions in the theta band at about 200 ms post-stimulus over

355   fronto-central electrodes across several asynchrony levels including AT70, AT20, and TA70.

356   These fronto-central AT interactions arose as a result of the AT+N power peak being weaker and

357   decaying earlier relative to the A+T sum. Critically, these fronto-central AT interactions for

358   theta power were most pronounced for ± 70 ms asynchrony levels, expressed less strongly for ±

359   20 ms and ± 500 ms asynchrony and completely absent for synchrony AT0 stimulation (see also

360   Figure 6d).

361   In addition, we observed significant AT interactions for theta power in the AT500 condition.

362   Specifically, in both early (60-600 ms) and late (610-1200 ms) time windows, AT interactions

363   were found with topographies that were distinct from the fronto-central P200-like theta-band

364   effects.

365   *Alpha/Beta power*: Because unisensory power changes and AT interactions were qualitatively

366   similar between the alpha and the low-beta bands, we combined these into one alpha/beta band

367   (8-20 Hz). Both tactile and auditory stimuli induced changes in the alpha/beta band primarily

368   over posterior channels (Figure 5, Unisensory row), which were more pronounced for tactile

369   stimulation. Auditory and tactile stimulation initially suppressed alpha/beta power (event-related

370   desynchronization; ERD) around 250 ms post-stimulation followed by a rebound (event-related

371   synchronisation; ERS) above and beyond baseline, around 800-1000 ms post-stimulation. This

372   alpha/beta power rebound was altered for AT + N relative to A + T across several asynchrony

373   levels including AT70, AT20, AT0, and TA70 conditions (Figure 2 for statistics and Figure 5).

374   Specifically, the rebound in alpha/beta power occurred earlier, was attenuated, and decayed

375   faster for AT+N than the A+T sum, where alpha/beta power rebound was found to be more

376   sustained (800-1100 ms post-stimulation).

377

378   **Summary of AT integration effects**

379   To provide an overview over the diverse AT interactions that we observed for ERPs, ITC, and

380   TF power, Figure 6 summarises the results, averaged over relevant spatial, temporal, and

381   frequency selections: the sum of the auditory and tactile (A+T; light blue), the sum of

382   audiotactile plus null (AT+N; dark blue) and the audiotactile interaction, i.e. the difference

383   [AT+N]-[A+V] as a function of AT asynchrony: 0, ±20, ±70, ±500 ms. This enables us to

384   characterise the profile of the AT interaction effects across asynchrony levels, including sub-

385   threshold effects in one asynchrony that relate to a significant effect in another asynchrony.

386   The early (~125 ms latency) AT interactions for ERPs followed an inverted U-shape function

387   that was constrained by a ≤20 ms TIW. They were significant only for AT0 and tapered off with

388   subthreshold effects at AT20 (Figure 6a).

389   The AT interactions for P200 in ERPs and theta band ITC at ~200 ms were significant

390   selectively for ± 70 ms AT asynchronies (Figure 6b and 6c). Surprisingly, the interactions for the

391   ERPs (i.e. P200) were symmetric and positive for both auditory and tactile leading asynchrony,

392   while the interactions for the ITC were asymmetric, i.e. negative for A leading and positive for T

393   leading asynchrony levels. This asymmetry and asynchrony specificity indicates that these ITC

394   effects are sensitive to the relative timing of the auditory and tactile signals - pointing towards

395   mechanisms of phase resetting.

396   The corresponding AT interactions for theta band TFP at ~200 ms post-stimulus were present

397   (at least at a sub-threshold level) across all AT asynchronies except for the physically

398   synchronous AT stimulation (Figure 6d). Specifically, we observed significant AT interactions

399   (i.e. reduction for AT+N relative to A+T) for AT500, AT70, AT20, and TA70 and non-

400   significant trends for TA20 and TA500.

401   The late AT interactions at ~400 ms latency for ERPs followed an inverted U-shape function

402   mimicking the response facilitation at the behavioural level (Figure 6e). These interactions were

403   significant for AT20 and TA20, with subthreshold effects for AT0, AT70, and TA70. Figure 3

404   shows that this late AT interaction emerges because the phase of the summed A+T response

405   ('trough') is in opposition to the phase of the summed AT+N response ('peak').

406   Finally, the late AT interactions for the alpha/beta band power "rebound" were observed

407   across several asynchronies (AT70, AT20, AT0, and TA70) (Figure 6f). They resulted from an

408   earlier occurrence and faster decay of the alpha/beta rebound for the AT+N compared to the sum

409   A + T and were most pronounced for A leading asynchronies (Figure 5).

410   To summarise, AT interactions were expressed across AT asynchrony levels with three

411   distinct profiles: i. inverted U-shape profile: early N100 and late 400 ms ERP effects, ii. most

412   pronounced for AT asynchronies of ±70 ms: ERP, ITC theta, and TFP theta effects at about 200

413   ms, and iii. most prominent for A leading asynchronies and present even outside the behavioural

414   TIW: late alpha/beta TFP rebound effects.

415

416   **Discussion**

417   The current study presented A, T, and AT stimuli at several asynchrony levels to investigate the

418   temporal constraints that govern behavioural response facilitation and neural AT interactions for

419   ERPs, ITC, and induced TF power.

420   Consistent with previous research (Colonius and Diederich, 2004), we observed an inverted

421   U-shape function for the behavioural AT benefit – also coined the redundant target effect

422   (Miller, 1982)- that was maximal for synchronous AT combinations and tapered off with

423   increasing AT asynchrony within a TIW of ≤70 ms (Zampini et al., 2005).

424   At the neural level we observed early AT interactions for evoked responses (ERP) at about

425   110 ms post-stimulus, which dovetails nicely with previous research showing multisensory

426   modulations of the N1 auditory component by visual and tactile stimuli (Foxe et al., 2000,

427   Lutkenhoner et al., 2002, Murray et al., 2005, Sperdin et al., 2009, Stekelenburg and Vroomen,

428   2009). Critically, our observed early AT interactions were sensitive to the relative timing of the

429   AT stimuli: they were most pronounced for synchronous AT stimuli and tapered off within a

430   small TIW of ≤20 ms. This temporal precision may be enhanced for interactions of tactile with

431   other sensory signals, because tactile latencies are fixed for a particular body location and do not

432   vary depending on the distance of the stimulus from the observer as in audition and vision. The

433   short latency and narrow temporal binding window points towards neural interactions in low

434   level or even primary auditory cortices that may rely on direct connectivity between sensory

435   areas (Fu et al., 2003, Cappe and Barone, 2005, de la Mothe et al., 2006a, Smiley et al., 2007) or

436   thalamic mechanisms (de la Mothe et al., 2006b, Hackett et al., 2007, Cappe et al., 2009) and

437   that increase the saliency of AT events leading to faster and more accurate detection.

438   Later, at about 400 ms post-stimulus, we observed audiotactile ERP interactions that were

439   again most pronounced for synchronous AT stimuli, but confined to a broader TIW of ≤70 ms,

440   which is consistent with a hierarchical organisation of AT interactions where early effects in low

441   level sensory areas are confined to a narrower temporal integration windows than later

442   interactions in association cortices (Hasson et al., 2008, Kiebel et al., 2008, Werner and

443   Noppeney, 2011). Moreover, the later interactions may in turn top-down modulate neural

444   processes in lower regions via feed-back loops (Falchier et al., 2002, Schroeder and Foxe, 2002,

445   Clavagnier et al., 2004). Both early and late ERP interactions followed an inverted U-shape

446   function thereby mimicking the temporal profile of the redundant target effect that characterised

447   observers' behaviour.

448   While the ERP effects at ~125 ms and ~400 ms post-stimulus were constrained by classical

449   temporal integration windows, the AT interactions for the P200 ERP component were most

450   pronounced for ± 70 ms AT asynchrony and absent for near-synchronous AT stimulation (see

451   Figure 3 and Figure 6b). Both the auditory and the tactile unisensory P200 are thought to be

452   generated in regions previously implicated in audiotactile integration (Foxe et al., 2002, Kayser

453   et al., 2005, Murray et al., 2005, Schurmann et al., 2006) such as the auditory belt area CM or

454   planum temporale (Godey et al., 2001, Crowley and Colrain, 2004, Smiley et al., 2007) and

455   secondary somatosensory areas (Forss et al., 1994, Disbrow et al., 2001), respectively. Our

456   results show that AT integration facilitates neural processing at about 200 ms post-stimulus: the

457   P200 peaks earlier, is smaller, and/or decays faster for the AT+N sum when compared to the sum

458   of the unisensory A and T conditions, consistent with multisensory literature, e.g. (Rowland et

459   al., 2007).

460   The P200 effects were also directly related to AT interactions for theta-band ITC that

461   emerged with a central topography again at ~200 ms post-stimulus selectively for ± 70 ms AT

462   asynchrony (compare Figures 6b and 6c). Critically, whilst the ERP interactions followed a

463   similar temporal profile and topography irrespective of whether the auditory or the tactile

464   stimulus is leading, the ITC effects were inverted for auditory relative to tactile leading

465   stimulation. This dissociation between ERP and ITC can be shown to occur in simulation

466   (https://github.com/johanna-zumer/audtac/blob/master/simulate_70results.m). The selectivity of

467   the P200 and the phase coherence effects for ± 70 ms AT asynchrony may be best accounted for

468   by mechanisms of phase resetting that have previously been implicated in audiotactile and

469   audiovisual interactions in auditory cortices (Lakatos et al., 2007, Kayser et al., 2008, Thorne et

470   al., 2011). From a functional perspective, a preceding tactile stimulus may reset the phase in

471   auditory cortices and thereby facilitate the localization of an auditory stimulus that is presented

472   70 ms later. Likewise, a preceding auditory stimulus may provide an alert to facilitate tactile

473   processing and possible avoidance actions. Not only have tones been shown to elicit responses

474   in somatosensory cortex (Borgest and Ermolaeva, 1975, Liang et al., 2013), but also an

475   *inhibitory* multisensory interaction by auditory stimulation was found in cat somatosensory area

476   SIV (Dehner et al., 2004) and auditory projections were found to inhibitory interneurons in cat

477   SIV (Keniston et al., 2010). In summary, our P200 and ITC results are supported by evidence of

478   bidirectional audiotactile integration, especially to association cortices, and of directional

479   asymmetries in the AT interaction (Cecere et al., 2017).

480   The AT interactions discussed so far were moulded by two distinct neural mechanisms: i.

481   ERP effects at ~100 and ~400 ms that followed an inverted U-shape function mimicking the

482   temporal binding window at the behavioural level and ii. P200 and theta ITC effects that were

483   selective for a particular level of AT asynchrony and may be mediated by mechanisms of phase

484   resetting. In contrast, AT interactions for induced theta oscillatory power were less specific and

485   expressed not only for $\pm$ 70 ms asynchrony, but across several asynchrony levels in particular

486   when the auditory stimulus was leading. While the topography and timing of the theta TF power

487   interactions *within* the TIW matched that of the P200 and ITC interactions, a distinct

488   topographical effect was found *outside* the classical behavioural integration window, in the

489   AT500 condition. Further, this enhanced oscillatory theta power was sustained until 1150 ms, i.e.

490   beyond the time needed to make a response in the redundant target paradigm of the associated

491   psychophysics study. We suggest that the AT theta power effects may reflect non-specific

492   mechanisms of multisensory priming or attention by which a preceding A signal may alert the

493   observer to imminent touch events, in light of the debate as to whether cross-modal stimuli with

494   asynchronies up to 500-600 ms may be actually *integrated* or whether the first stimulus (only)

495   primes and/or draws exogenous (spatial) cross-modal attention (Macaluso et al., 2001,

496   McDonald et al., 2001, Stein et al., 2010). Alternatively, the AT500 condition may be viewed as

497   a type of "No-go" trial in which a response to the second stimulus is to be withheld, which has

498   previously been shown to be associated with frontal theta oscillations (Kirmizi-Alsan et al.,

499   2006, Harper et al., 2014).

500   Likewise, we observed AT interactions for alpha/beta oscillatory power at ~1000 ms post-

501   stimulus. As shown in Figure 5, both auditory and tactile stimuli suppressed alpha/beta

502   oscillatory power (event-related desynchronization; ERD) at about 200-400 ms, related to a

503   release from inhibition, followed by a rebound in power beyond baseline levels from about 600

504   ms – 1200 ms post-stimulus (event-related synchronisation; ERS), related to resetting and

505   recovery (Pfurtscheller and Lopes da Silva, 1999, Neuper and Pfurtscheller, 2001). Our results

506   show that the initial suppression (ERD) of alpha/beta power is not significantly different from

507   the sum of the auditory and tactile induced suppressions; yet, the rebound in alpha/beta power for

508   the AT+Null sum is weaker and decays faster than predicted by the A+T sum of the additive

509   model. Further, we observed significant AT interactions for the alpha/beta rebound for AT70,

510   AT20, AT0, and TA70, and as a non-significant trend for the AT500 asynchrony level. Because

511   the AT interactions of power rebound occurred after the explicit detection response is made by

512   participants in the redundant target paradigm, it may be a consequence of the implicit AT event

513   detection, or be associated with post-decisional processes such as metacognitive monitoring

514   (Deroy et al., 2016), or the binding of asynchronous signals into a single multisensory percept

515   (Roa Romero et al., 2015). Future redundant target paradigms that combine target detection with

516   post-decisional tasks (e.g. confidence judgments) may enable us to further determine the

517   functional role of the alpha/beta rebound and the associated AT interactions. The distinct

518   response profile for theta versus alpha/beta power, varying with stimulus asynchrony, is in line

519   with distinct mechanisms for different frequencies (Keil and Senkowski, 2018).

520   To conclude, this psychophysics-EEG study unravels a multitude of neural interactions, which

521   arose with different temporal constraints: interactions were confined to a TIW for ERPs, specific

522   for one particular asynchrony for inter-trial coherence, and extending beyond the behavioural

523   TIW for induced low frequency power. This diversity of temporal profiles demonstrates that

524   distinct neural mechanisms govern a cascade of multisensory integration processes.

525

526   **References:**

527   Atilgan H, Town SM, Wood KC, Jones GP, Maddox RK, Lee AKC, Bizley JK (2018)

528   Integration of Visual Information in Auditory Cortex Promotes Auditory Scene Analysis

529   through Multisensory Binding. Neuron 97:640-655 e644.

530   Berger CC, Ehrsson HH (2014) The fusion of mental imagery and sensation in the temporal

531   association cortex. J Neurosci 34:13684-13692.

532   Bizley JK, Nodal FR, Bajo VM, Nelken I, King AJ (2007) Physiological and anatomical

533   evidence for multisensory interactions in auditory cortex. Cereb Cortex 17:2172-2189.

534   Blurton SP, Greenlee MW, Gondan M (2015) Cross-modal cueing in audiovisual spatial

535   attention. Atten Percept Psychophys 77:2356-2376.

536   Borgest AN, Ermolaeva V (1975) [Functional organization of pathways transmitting auditory

537   signals in the somatosensory zone of the cat cerebral cortex]. Neirofiziologiia 7:476-485.

538   Cappe C, Barone P (2005) Heteromodal connections supporting multisensory integration at low

539   levels of cortical processing in the monkey. Eur J Neurosci 22:2886-2902.

540   Cappe C, Morel A, Barone P, Rouiller EM (2009) The thalamocortical projection systems in

541   primate: an anatomical support for multisensory and sensorimotor interplay. Cereb

542   Cortex 19:2025-2037.

543   Cecere R, Gross J, Willis A, Thut G (2017) Being First Matters: Topographical Representational

544   Similarity Analysis of ERP Signals Reveals Separate Networks for Audiovisual

545   Temporal Binding Depending on the Leading Sense. J Neurosci 37:5274-5287.

546   Clavagnier S, Falchier A, Kennedy H (2004) Long-distance feedback projections to area V1:

547   implications for multisensory integration, spatial awareness, and visual consciousness.

548   Cogn Affect Behav Neurosci 4:117-126.

549   Colonius H, Diederich A (2004) Multisensory interaction in saccadic reaction time: a time-

550   window-of-integration model. J Cogn Neurosci 16:1000-1009.

551   Crowley KE, Colrain IM (2004) A review of the evidence for P2 being an independent

552   component process: age, sleep and modality. Clin Neurophysiol 115:732-744.

553   Dahl CD, Logothetis NK, Kayser C (2009) Spatial organization of multisensory responses in

554   temporal association cortex. J Neurosci 29:11924-11932.

555   de la Mothe LA, Blumell S, Kajikawa Y, Hackett TA (2006a) Cortical connections of the

556   auditory cortex in marmoset monkeys: core and medial belt regions. J Comp Neurol

557   496:27-71.

558   de la Mothe LA, Blumell S, Kajikawa Y, Hackett TA (2006b) Thalamic connections of the

559   auditory cortex in marmoset monkeys: core and medial belt regions. J Comp Neurol

560   496:72-96.

561   Dehner LR, Keniston LP, Clemo HR, Meredith MA (2004) Cross-modal circuitry between

562   auditory and somatosensory areas of the cat anterior ectosylvian sulcal cortex: a 'new'

563   inhibitory form of multisensory convergence. Cereb Cortex 14:387-403.

564   Deroy O, Spence C, Noppeney U (2016) Metacognition in Multisensory Perception. Trends

565   Cogn Sci 20:736-747.

566   Diederich A, Colonius H (2004) Bimodal and trimodal multisensory enhancement: effects of

567   stimulus onset and intensity on reaction time. Percept Psychophys 66:1388-1404.

568   Disbrow E, Roberts T, Poeppel D, Krubitzer L (2001) Evidence for interhemispheric processing

569   of inputs from the hands in human S2 and PV. J Neurophysiol 85:2236-2244.

570   Donohue SE, Green JJ, Woldorff MG (2015) The effects of attention on the temporal integration

571   of multisensory stimuli. Front Integr Neurosci 9:32.

572   Downar J, Crawley AP, Mikulis DJ, Davis KD (2000) A multimodal cortical network for the

573   detection of changes in the sensory environment. Nat Neurosci 3:277-283.

574   Falchier A, Clavagnier S, Barone P, Kennedy H (2002) Anatomical evidence of multimodal

575   integration in primate striate cortex. J Neurosci 22:5749-5759.

576   Fetsch CR, Pouget A, DeAngelis GC, Angelaki DE (2011) Neural correlates of reliability-based

577   cue weighting during multisensory integration. Nat Neurosci 15:146-154.

578   Forss N, Salmelin R, Hari R (1994) Comparison of somatosensory evoked fields to airpuff and

579   electric stimuli. Electroencephalogr Clin Neurophysiol 92:510-517.

580   Foxe JJ, Morocz IA, Murray MM, Higgins BA, Javitt DC, Schroeder CE (2000) Multisensory

581   auditory-somatosensory interactions in early cortical processing revealed by high-density

582   electrical mapping. Brain Res Cogn Brain Res 10:77-83.

583   Foxe JJ, Schroeder CE (2005) The case for feedforward multisensory convergence during early

584   cortical processing. Neuroreport 16:419-423.

585   Foxe JJ, Wylie GR, Martinez A, Schroeder CE, Javitt DC, Guilfoyle D, Ritter W, Murray MM

586   (2002) Auditory-somatosensory multisensory processing in auditory association cortex:

587   an fMRI study. J Neurophysiol 88:540-543.

588   Fu KM, Johnston TA, Shah AS, Arnold L, Smiley J, Hackett TA, Garraghty PE, Schroeder CE

589   (2003) Auditory cortical neurons respond to somatosensory stimulation. J Neurosci

590   23:7510-7515.

591   Ghazanfar AA, Schroeder CE (2006) Is neocortex essentially multisensory? Trends Cogn Sci

592   10:278-285.

593   Giard MH, Peronnet F (1999) Auditory-visual integration during multimodal object recognition

594   in humans: a behavioral and electrophysiological study. J Cogn Neurosci 11:473-490.

595   Godey B, Schwartz D, de Graaf JB, Chauvel P, Liegeois-Chauvel C (2001) Neuromagnetic

596   source localization of auditory evoked fields and intracerebral evoked potentials: a

597   comparison of data in the same patients. Clin Neurophysiol 112:1850-1859.

598   Hackett TA, De La Mothe LA, Ulbert I, Karmos G, Smiley J, Schroeder CE (2007) Multisensory

599   convergence in auditory cortex, II. Thalamocortical connections of the caudal superior

600   temporal plane. J Comp Neurol 502:924-952.

601   Harper J, Malone SM, Bernat EM (2014) Theta and delta band activity explain N2 and P3 ERP

602   component activity in a go/no-go task. Clin Neurophysiol 125:124-132.

603   Harrar V, Harris LR (2008) The effect of exposure to asynchronous audio, visual, and tactile

604   stimulus combinations on the perception of simultaneity. Exp Brain Res 186:517-524.

605   Hasson U, Yang E, Vallines I, Heeger DJ, Rubin N (2008) A hierarchy of temporal receptive

606   windows in human cortex. J Neurosci 28:2539-2550.

607   Hershenson M (1962) Reaction time as a measure of intersensory facilitation. J Exp Psychol

608   63:289-293.

609   Hoefer M, Tyll S, Kanowski M, Brosch M, Schoenfeld MA, Heinze HJ, Noesselt T (2013)

610   Tactile stimulation and hemispheric asymmetries modulate auditory perception and

611   neural responses in primary auditory cortex. Neuroimage 79:371-382.

612   Ibrahim LA, Mesik L, Ji XY, Fang Q, Li HF, Li YT, Zingg B, Zhang LI, Tao HW (2016) Cross-

613   Modality Sharpening of Visual Cortical Processing through Layer-1-Mediated Inhibition

614   and Disinhibition. Neuron 89:1031-1045.

615   Kayser C, Petkov CI, Augath M, Logothetis NK (2005) Integration of touch and sound in

616   auditory cortex. Neuron 48:373-384.

617   Kayser C, Petkov CI, Augath M, Logothetis NK (2007) Functional imaging reveals visual

618   modulation of specific fields in auditory cortex. J Neurosci 27:1824-1835.

619   Kayser C, Petkov CI, Logothetis NK (2008) Visual modulation of neurons in auditory cortex.

620   Cereb Cortex 18:1560-1574.

621   Keil J, Senkowski D (2018) Neural Oscillations Orchestrate Multisensory Processing.

622   Neuroscientist 1073858418755352.

623   Keniston LP, Henderson SC, Meredith MA (2010) Neuroanatomical identification of crossmodal

624   auditory inputs to interneurons in somatosensory cortex. Exp Brain Res 202:725-731.

625   Kiebel SJ, Daunizeau J, Friston KJ (2008) A hierarchy of time-scales and the brain. PLoS

626   Comput Biol 4:e1000209.

627   Kirmizi-Alsan E, Bayraktaroglu Z, Gurvit H, Keskin YH, Emre M, Demiralp T (2006)

628   Comparative analysis of event-related potentials during Go/NoGo and CPT:

629   decomposition of electrophysiological markers of response inhibition and sustained

630   attention. Brain Res 1104:114-128.

631   Lakatos P, Chen CM, O'Connell MN, Mills A, Schroeder CE (2007) Neuronal oscillations and

632   multisensory interaction in primary auditory cortex. Neuron 53:279-292.

633   Leclercq Y, Schrouff J, Noirhomme Q, Maquet P, Phillips C (2011) fMRI artefact rejection and

634   sleep scoring toolbox. Comput Intell Neurosci 2011:598206.

635   Leonardelli E, Braun C, Weisz N, Lithari C, Occelli V, Zampini M (2015) Prestimulus

636   oscillatory alpha power and connectivity patterns predispose perceptual integration of an

637   audio and a tactile stimulus. Hum Brain Mapp 36:3486-3498.

638   Liang M, Mouraux A, Hu L, Iannetti GD (2013) Primary sensory cortices contain distinguishable

639   spatial patterns of activity for each sense. Nat Commun 4:1979.

640   Lutkenhoner B, Lammertmann C, Simoes C, Hari R (2002) Magnetoencephalographic correlates

641   of audiotactile interaction. Neuroimage 15:509-522.

642   Macaluso E, Frith C, Driver J (2001) (Response to) Multisensory Integration and Crossmodal

643   Attention Effects in the Human Brain. Science 292:1791-1791.

644   McDonald JJ, Teder-Sälejärvi WA, Ward LM (2001) Multisensory Integration and Crossmodal

645   Attention Effects in the Human Brain. Science 292:1791-1791.

646   Megevand P, Molholm S, Nayak A, Foxe JJ (2013) Recalibration of the multisensory temporal

647   window of integration results from changing task demands. PLoS One 8:e71608.

648   Mercier MR, Foxe JJ, Fiebelkorn IC, Butler JS, Schwartz TH, Molholm S (2013) Auditory-

649   driven phase reset in visual cortex: human electrocorticography reveals mechanisms of

650   early multisensory integration. Neuroimage 79:19-29.

651   Mercier MR, Molholm S, Fiebelkorn IC, Butler JS, Schwartz TH, Foxe JJ (2015) Neuro-

652   oscillatory phase alignment drives speeded multisensory response times: an electro-

653   corticographic investigation. J Neurosci 35:8546-8557.

654   Meredith MA, Stein BE (1983) Interactions among converging sensory inputs in the superior

655   colliculus. Science 221:389-391.

656   Miller J (1982) Divided attention: evidence for coactivation with redundant signals. Cogn

657   Psychol 14:247-279.

658   Molholm S, Ritter W, Murray MM, Javitt DC, Schroeder CE, Foxe JJ (2002) Multisensory
659   auditory-visual interactions during early sensory processing in humans: a high-density
660   electrical mapping study. Brain Res Cogn Brain Res 14:115-128.

661   Murray MM, Molholm S, Michel CM, Heslenfeld DJ, Ritter W, Javitt DC, Schroeder CE, Foxe
662   JJ (2005) Grabbing your ear: rapid auditory-somatosensory multisensory interactions in
663   low-level sensory cortices are not constrained by stimulus alignment. Cereb Cortex
664   15:963-974.

665   Navarra J, Soto-Faraco S, Spence C (2007) Adaptation to audiotactile asynchrony. Neurosci Lett
666   413:72-76.

667   Neuper C, Pfurtscheller G (2001) Event-related dynamics of cortical rhythms: frequency-specific
668   features and functional correlates. Int J Psychophysiol 43:41-58.

669   Nishi A, Yokoyama M, Ogawa K, Ogata T, Nozawa T, Miyake Y (2014) Effects of Voluntary
670   Movements on Audio-Tactile Temporal Order Judgment. Ieice T Inf Syst E97d:1567-
671   1573.

672   Oostenveld R, Fries P, Maris E, Schoffelen JM (2011) FieldTrip: Open source software for
673   advanced analysis of MEG, EEG, and invasive electrophysiological data. Comput Intell
674   Neurosci 2011:156869.

675   Pfurtscheller G, Lopes da Silva FH (1999) Event-related EEG/MEG synchronization and
676   desynchronization: basic principles. Clin Neurophysiol 110:1842-1857.

677   Roa Romero Y, Senkowski D, Keil J (2015) Early and late beta-band power reflect audiovisual
678   perception in the McGurk illusion. J Neurophysiol 113:2342-2350.

679   Rohe T, Noppeney U (2015) Cortical hierarchies perform Bayesian causal inference in
680   multisensory perception. PLoS Biol 13:e1002073.

681   Rohe T, Noppeney U (2016) Distinct Computational Principles Govern Multisensory Integration

682   in Primary Sensory and Association Cortices. Curr Biol 26:509-514.

683   Rowland BA, Quessy S, Stanford TR, Stein BE (2007) Multisensory integration shortens

684   physiological response latencies. J Neurosci 27:5879-5884.

685   Rowland BA, Stein BE (2007) Multisensory integration produces an initial response

686   enhancement. Front Integr Neurosci 1:4.

687   Schroeder CE, Foxe JJ (2002) The timing and laminar profile of converging inputs to

688   multisensory areas of the macaque neocortex. Brain Res Cogn Brain Res 14:187-198.

689   Schurmann M, Caetano G, Hlushchuk Y, Jousmaki V, Hari R (2006) Touch activates human

690   auditory cortex. Neuroimage 30:1325-1331.

691   Senkowski D, Gomez-Ramirez M, Lakatos P, Wylie GR, Molholm S, Schroeder CE, Foxe JJ

692   (2007) Multisensory processing and oscillatory activity: analyzing non-linear

693   electrophysiological measures in humans and simians. Exp Brain Res 177:184-195.

694   Senkowski D, Schneider TR, Foxe JJ, Engel AK (2008) Crossmodal binding through neural

695   coherence: implications for multisensory processing. Trends Neurosci 31:401-409.

696   Smiley JF, Hackett TA, Ulbert I, Karmas G, Lakatos P, Javitt DC, Schroeder CE (2007)

697   Multisensory convergence in auditory cortex, I. Cortical connections of the caudal

698   superior temporal plane in macaque monkeys. J Comp Neurol 502:894-923.

699   Sperdin HF, Cappe C, Foxe JJ, Murray MM (2009) Early, low-level auditory-somatosensory

700   multisensory interactions impact reaction time speed. Front Integr Neurosci 3:2.

701   Stanford TR, Quessy S, Stein BE (2005) Evaluating the operations underlying multisensory

702   integration in the cat superior colliculus. J Neurosci 25:6499-6508.

703   Stein BE, Burr D, Constantinidis C, Laurienti PJ, Alex Meredith M, Perrault TJ, Jr.,

704   Ramachandran R, Roder B, Rowland BA, Sathian K, Schroeder CE, Shams L, Stanford

705   TR, Wallace MT, Yu L, Lewkowicz DJ (2010) Semantic confusion regarding the

706   development of multisensory integration: a practical solution. Eur J Neurosci 31:1713-

707   1720.

708   Stekelenburg JJ, Vroomen J (2009) Neural correlates of audiovisual motion capture. Exp Brain

709   Res 198:383-390.

710   Thorne JD, De Vos M, Viola FC, Debener S (2011) Cross-modal phase reset predicts auditory

711   task performance in humans. J Neurosci 31:3853-3861.

712   van Wassenhove V, Grant KW, Poeppel D (2007) Temporal window of integration in auditory-

713   visual speech perception. Neuropsychologia 45:598-607.

714   Werner S, Noppeney U (2010a) Distinct functional contributions of primary sensory and

715   association areas to audiovisual integration in object categorization. J Neurosci 30:2662-

716   2675.

717   Werner S, Noppeney U (2010b) Superadditive responses in superior temporal sulcus predict

718   audiovisual benefits in object categorization. Cereb Cortex 20:1829-1842.

719   Werner S, Noppeney U (2011) The contributions of transient and sustained response codes to

720   audiovisual integration. Cereb Cortex 21:920-931.

721   Zampini M, Brown T, Shore DI, Maravita A, Roder B, Spence C (2005) Audiotactile temporal

722   order judgments. Acta Psychol (Amst) 118:277-291.

723

724

725   **Legends**

726   **Figure 1.** Experimental design, behavioural results, and evoked responses. *a,* Each row depicts

727   the onsets of the auditory stimulation (indicated by loudspeaker) and tactile stimulation

728   (indicated by face) for each of the 10 conditions including the null (N), auditory alone (A), tactile

729   alone (T) and the seven AT conditions with asynchrony: 0, ±20, ±70, and ±500 ms. The wavy

730   line at the bottom indicates the continuous MRI background noise. *b,* Reaction times (across

731   subjects' mean ± SEM). The black lines indicate the AT conditions as a function of AT

732   asynchrony with negative asynchronies indicating auditory-leading; the green and pink bars

733   indicate the A and T conditions, respectively. *c,* Evoked response potentials for N, A, T, and AT

734   conditions for frontocentral ['Fz' 'Cz' 'F1' 'F2' 'FC1' 'FC2' 'C1' 'C2'] and posterior ['CP5' 'POz' 'Pz'

735   'P3' 'P4' 'C4' 'O1' 'O2' 'P7' 'PO7'] sets of sensors. The A evoked response is shifted by the

736   appropriate asynchrony to align with the auditory onset in the corresponding AT condition.

737

738   **Figure 2**: Statistics for behavioural and neural results for each AT asynchrony (rows).

739   *Behavioural redundant target effect (RTE)*: paired t-tests (sample size: N=22; degrees of

740   freedom = 21) comparing the AT response time with the minimal unisensory response time. For

741   AT500 the AT response was slower than the minimal unisensory response (negative t-value).

742   The "e" indicates "x 10^". *Neural AT interactions* [(A+T) – (AT + N)] for ERPs (blue), ITC

743   (violet), and TFP (red) listed in separate columns for different latency ranges: non-parametric

744   permutation dependent/paired samples t-tests (sample size N=22) comparing A+T with AT+N.

745   The p-values are reported at the cluster level (max sum) corrected for multiple comparisons over

746   channels and time (and frequency for ITC and TFP) with an auxiliary uncorrected threshold of

747   p<0.05. P-values in italics indicate a non-significant trend.

748

749   **Figure 3.** Evoked response potentials. Each row shows the audiotactile interaction for a

750   particular level of AT asynchrony. (A) ERPs of the sum of the auditory and tactile (A+T; light

751   blue), the sum of audiotactile plus null (AT+N; dark blue), and the audiotactile interaction, i.e.

752   the difference ([A+T]-[AT+N], orange). Green = auditory onset, pink = tactile onset. Shaded

753   grey areas indicate the timing of significant AT interactions at $p < 0.05$ corrected at the cluster

754   level for multiple comparisons across electrodes and time points within a 500 ms window

755   starting with the second stimulus and limited by the black dashed line. (B) Topographies of the

756   sums: A+T, AT+N, and (A+T)-(AT+N) for time windows of significant AT interactions. The

757   time windows written in orange are relative to the onset of the second stimulus. A black star over

758   an electrode indicates that it is part of a significant cluster.

759

760   **Figure 4.** Inter-trial coherence. Each row shows the audiotactile interaction in the ITC for a

761   particular level of AT asynchrony, plus the unisensory conditions. (A) ITC of the sum of the

762   auditory and tactile (A+T; light blue), the sum of audiotactile plus null (AT+N; dark blue), and

763   the audiotactile interaction, i.e. the difference ([A+T]-[AT+N], orange). The bottom row shows

764   the Null (grey), Tactile (pink), and Auditory (green) conditions. Green = auditory onset, pink =

765   tactile onset. Shaded grey areas indicate the timing of significant AT interactions at $p < 0.05$

766   corrected at the cluster level for multiple comparisons across electrodes, frequency, and time

767   points within a 1200 ms window starting with the second stimulus and limited by the black

768   dashed line. (B) Topographies of the sums: A+T, AT+N, and (A+T)-(AT+N) for time windows

769   of significant AT interactions. The time windows written in orange are relative to the onset of the

770   second stimulus. A black star over an electrode indicates that it is part of a significant cluster.

771

772   **Figure 5.** Time-frequency power. Each row shows the audiotactile interaction for a particular

773   level of AT asynchrony. (A) Theta and (B) Alpha/Beta power of the sum of the auditory and

774   tactile (A+T; light blue), the sum of audiotactile plus null (AT+N; dark blue), and the

775   audiotactile interaction, i.e. the difference ([A+T]-[AT+N], orange). The bottom row shows the

776   null (grey), tactile (pink), and auditory (green) condition. Green = auditory onset, pink = tactile

777   onset. Shaded grey areas indicate the timing of significant AT interactions at $p < 0.05$ corrected

778   at the cluster level for multiple comparisons across electrodes, frequency, and time points within

779   a 1200 ms window starting with the second stimulus and limited by the black dashed line. (C)

780   Topographies of the sums: A+T, AT+N, and (A+T)-(AT+N) for time windows of significant AT

781   interactions, arranged in the same way as in Figures 3 and 4. The time windows written in orange

782   are relative to the onset of the second stimulus. A black star over an electrode indicates that it is

783   part of a significant cluster.

784

785   **Figure 6**: Summary of six audiotactile interactions (rows a-f) for ERP, ITC, and TFP across the

786   seven asynchrony levels. *Left:* Topographies of ERP, ITC, or TFP (as indicated), centred around

787   a post-stimulus time (as indicated ± 20 ms), for a particular AT asynchrony level (as indicated in

788   orange). *Right*: Line plots showing ERP, ITC, or TFP of the sum of the auditory and tactile

789   (A+T; light blue), the sum of audiotactile plus null (AT+N; dark blue), and the audiotactile

790   interaction, i.e. the difference ([A+T]-[AT+N]; orange) as a function of AT asynchrony: 0, ±20,

791   ±70, and ±500 ms. The values are averaged across the representative electrodes highlighted in

792   the topographies (left) and within a 40 ms time window centred on the latencies specified

793   alongside the corresponding topographies. For interpretational purposes, the labels 'U' and '70'

794   indicate via colour coding whether 'A+T' and 'AT+N' (blue) or the AT interaction (orange)

795   follow a U-shape function (= U) or are selective for ±70 ms asynchrony (= 70).

a Trial type schematic
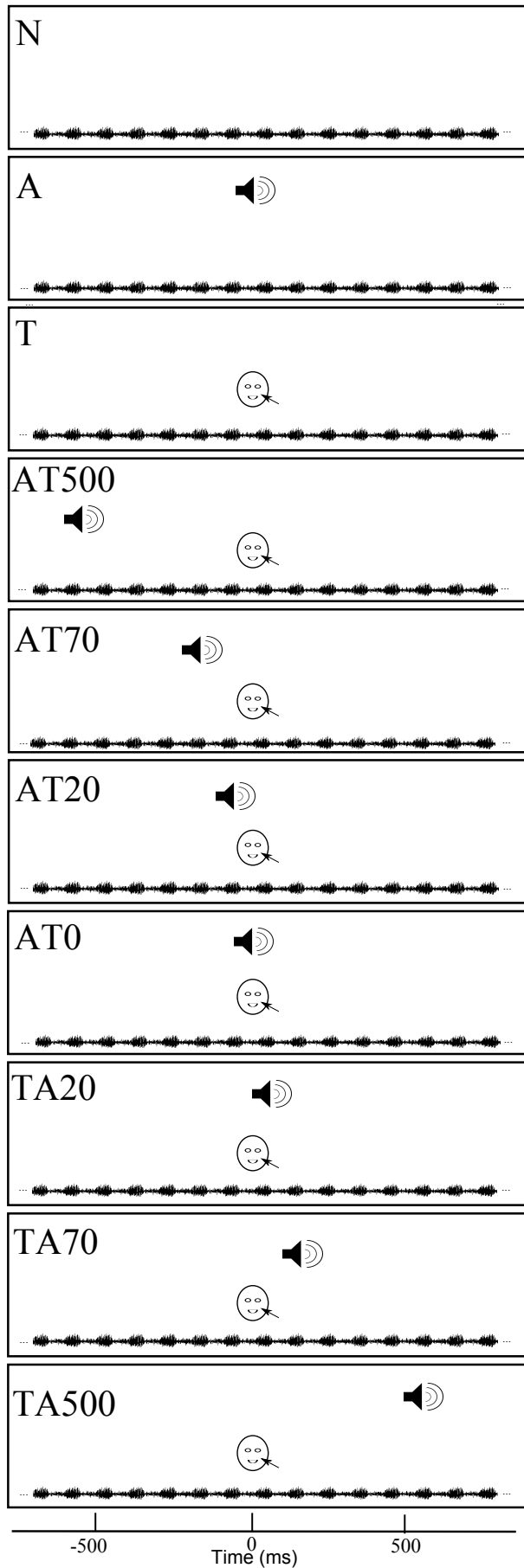
b Reaction times by AT asynchrony
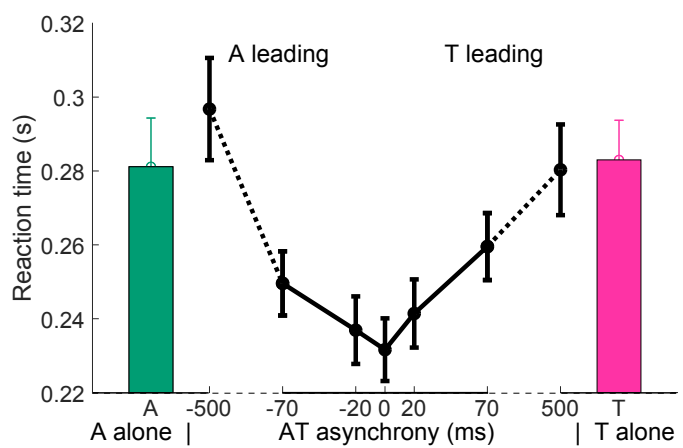
c Evoked response potentials
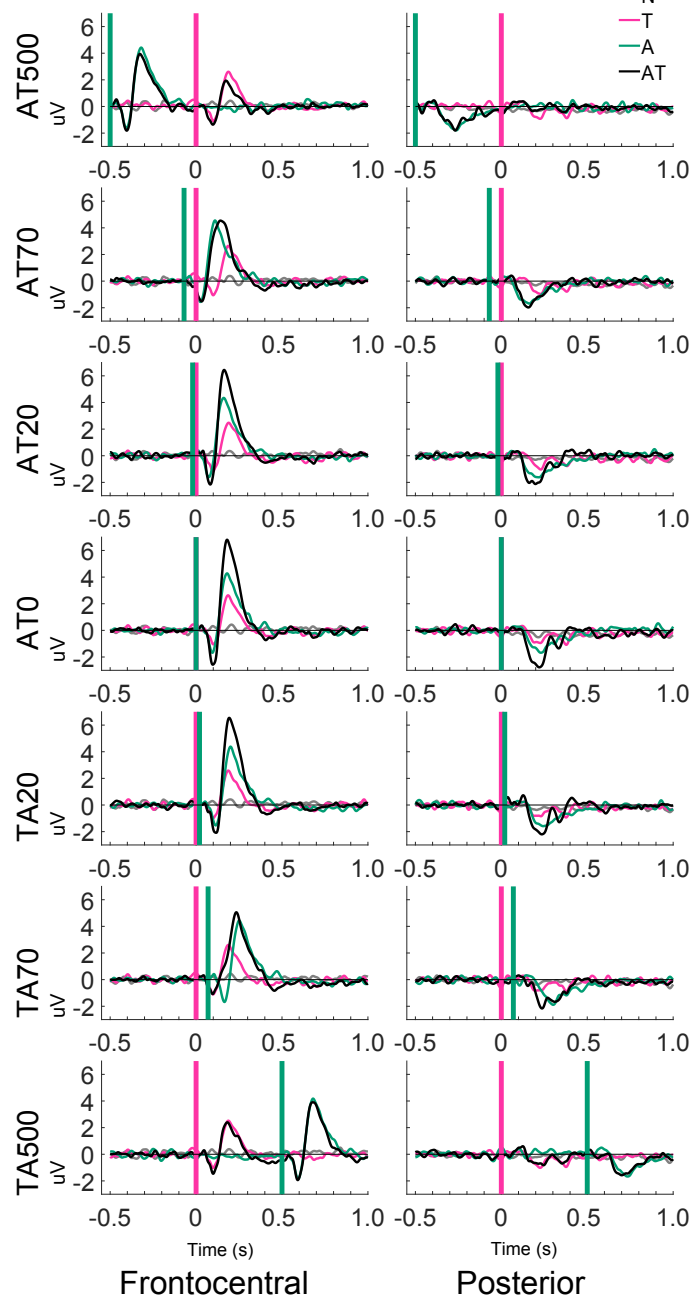
| MSI effects Asynchrony:	Behaviour: RTE	Neural Post-stimulus Latency: ~125 ms	~200 ms	~400 ms	~800-1100 ms
AT500	p=0.001 t=3.7				β TFP 860-1150 ms (p=0.014)
AT70	p=1.2e-5 t=5.7		ERP 120-270 ms (p=0.010) θ ITC 0-260 ms (p=0.037) θ TFP 90-640 ms (p=0.01)		β TFP 1030-1150 ms (p=0.042)
AT20	p=7.2e-8 t=8.1	ERP 40-100 ms (p=0.072)	θ TFP 0-470 ms (p=0.049)	ERP 370-420 ms (p=0.022)	α & β TFP 700-1000 ms (p=0.027)
AT0	p=1.1e-7 t=7.8	ERP 70-170 ms (p=0.017)		ERP 370-420 ms (p=0.28)	α & β TFP 840-1140 ms (p=0.017)
TA20	p=2.1e-8 t=8.7			ERP 340-400 ms (p=0.03)	
TA70	p=8.8e-5 t=4.8		ERP 140-220 ms (p=0.007) θ ITC 0-490 ms (p=0.0005) θ TFP 0-480 ms (p=0.005)		α/β TFP 870-1200 ms (p=0.023)
TA500					

ERP: AT interactions as a function of AT asynchrony

a

Frontocentral   Posterior

b   Topgraphy

120-270 ms

370-420 ms

70-170 ms

340-400 ms

140-220 ms

Post-tactile stimulus time (s)

A+T
AT+N
(A+T)-(AT+N)
T onset
A onset
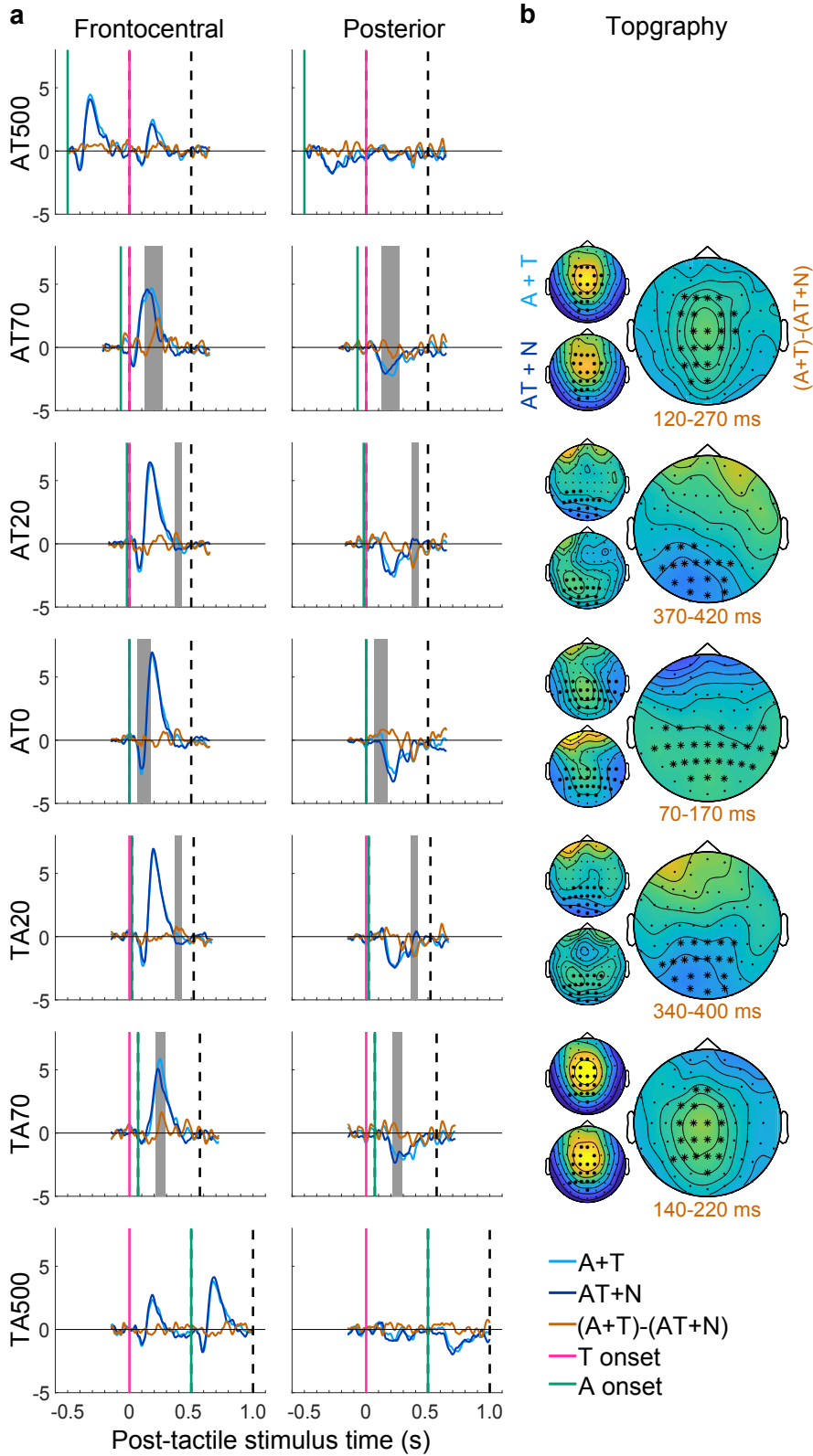
Inter-trial coherence (Theta; 4-8 Hz):
AT interactions as a function of AT asynchrony
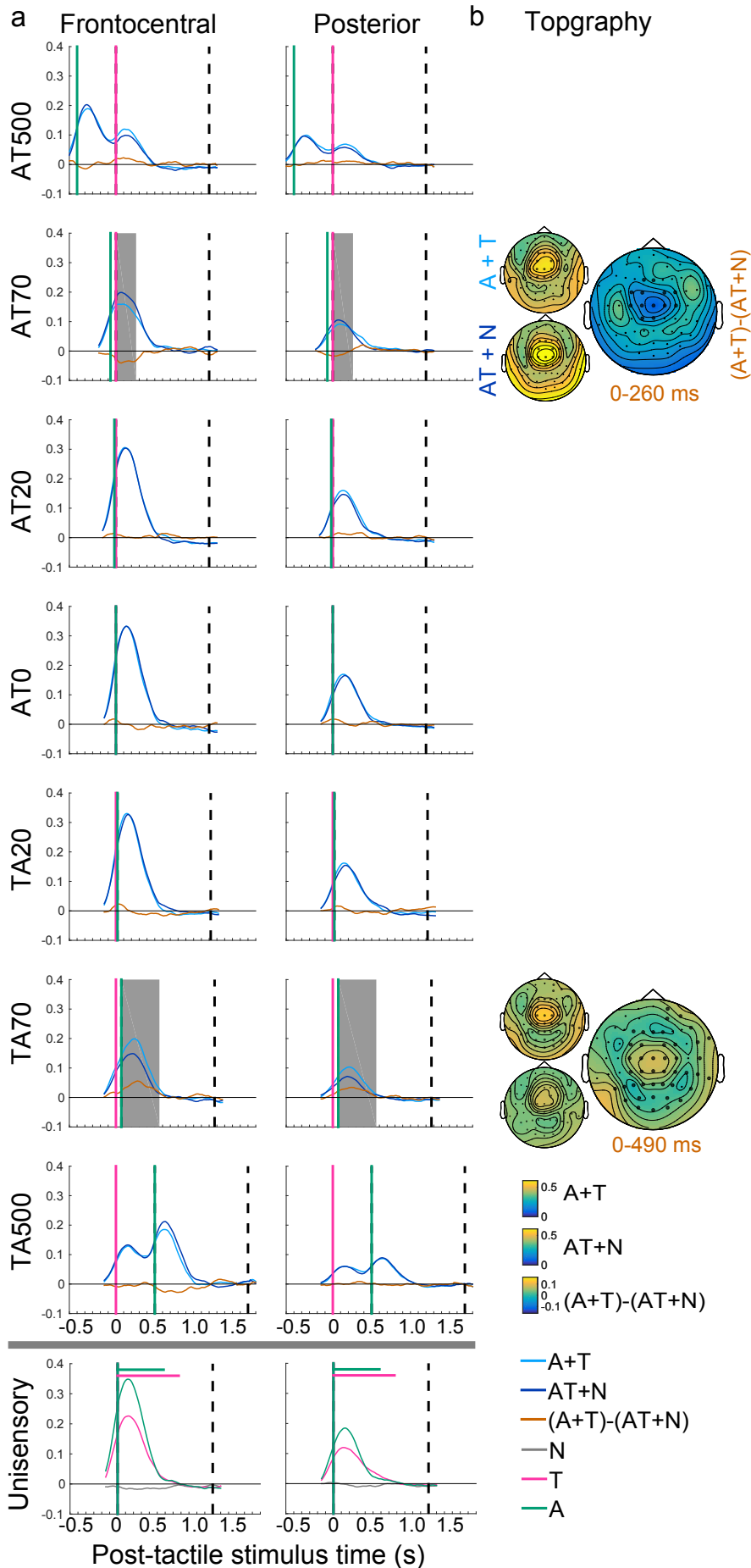
Time-frequency power: AT interactions as a function of AT asynchrony
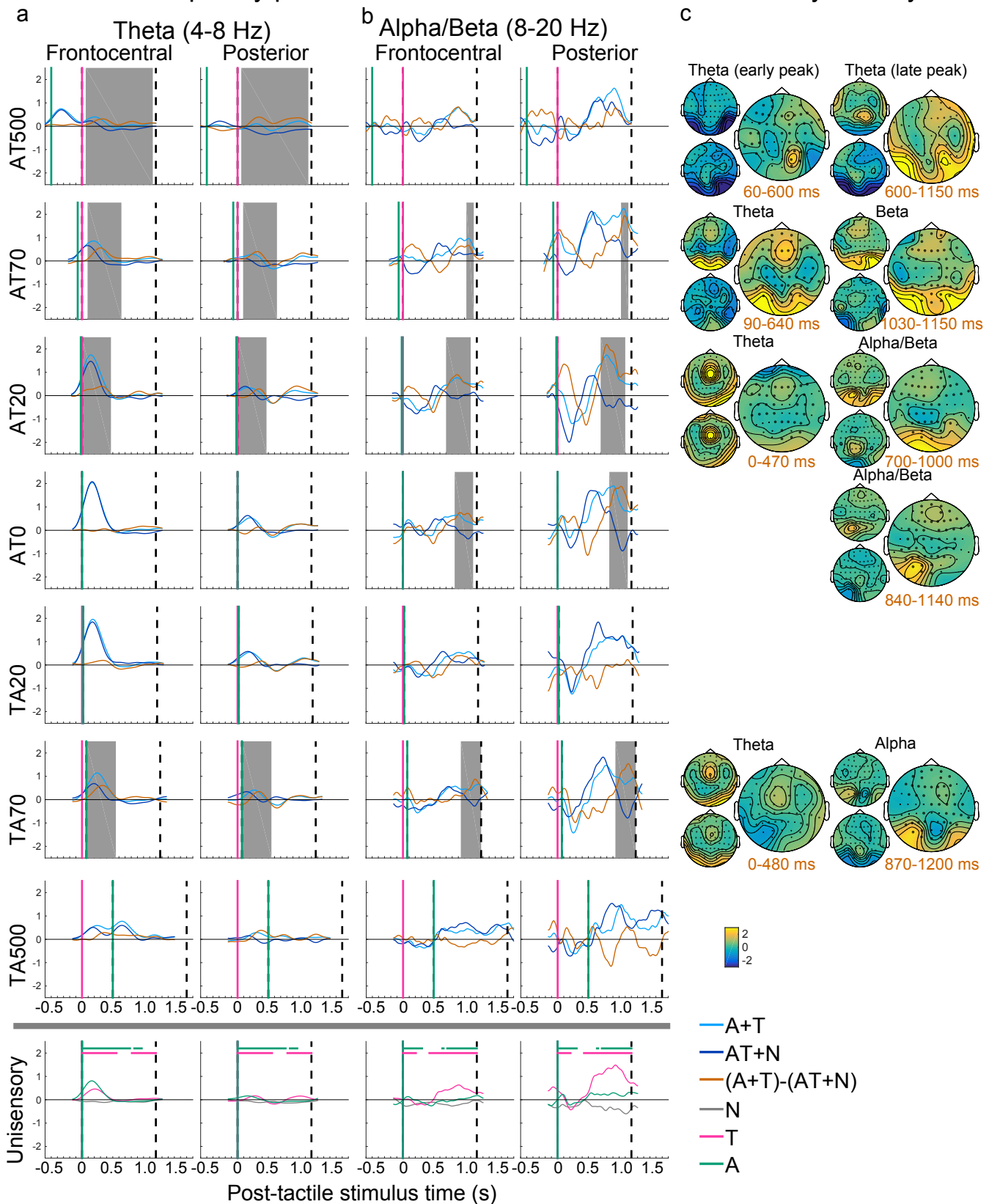
Summary of audiotactile interactions